0273-2289/00/88/0077/$15.00

Structural Determinants for the Efficient and Specific Interaction of Thioredoxin with 2-Oxoacid Dehydrogenase Complexes

GUENTER RADDATZ,[1] VOLKER KRUFT,[2] AND VICTORIA BUNIK*,[3]

[1]Institute of Physiological Chemistry, Tuebingen University, D-72076 Tuebingen, Germany; [2]Perkin Elmer Applied Biosystems, European Life Science Center, D-63225 Langen, Germany; and [3]A. N. Belozersky Institute of Physico-Chemical Biology, Moscow State University, Moscow 119899, Russia, E-mail: vbun@bac.genebee.msu.su

Abstract

Specificity and efficiency of thioredoxin action upon the 2-oxoacid dehydrogenase complexes are studied by using a number of thioredoxins and complexes. Bacterial and mammalian pyruvate and 2-oxoglutarate dehydrogenase systems display similar row of preference to thioredoxins that may result from thioredoxin binding to the homologous or common dihydrolipoamide dehydrogenase components of the complexes. The most sensitive to thioredoxin is the complex whose component exhibits the highest sequence similarity to eukaryotic thioredoxin reductase. Hence, thioredoxin binding to the complexes may be related to that in the thioredoxin reductase, a dihydrolipoamide dehydrogenase homolog. The highest potency of mitochondrial thioredoxin to affect the mitochondrial complexes is revealed. A 96–100% conservation of the mitochondrial thioredoxin structure is shown within the four known sequences and the N-terminus of the pig heart protein determined. Eleven thioredoxins tested biochemically are analyzed by multiple sequence alignment and homology modeling. Their effects correlate with the residues at the contact between the $\alpha 3/3_{10}$ and $\alpha 1$ helices, the length of the $\alpha 1$ helix and charges in the $\alpha 2$–$\beta 3$ and $\beta 4$–$\beta 5$ linkers. Polarization of the thioredoxin molecule and its active site surroundings are characterized. Thioredoxins with a highly polarized surface around the essential disulfide bridge (mitochondrial, pea *f*, and *Arabidopsis thaliana h3*) show low cross-reactivity as compared to the species with a decreased polarization of this area (e.g., from *Escherichia coli)*. The strongest polarization of the whole molecule results in the highest magnitude of the electrostatic dipole vector of mitochondrial thioredoxin. Thioredoxins with the dipole orientation similar to that of the latter have the affinities for the 2-oxoacid dehydrogenase

*Author to whom all correspondence and reprint requests should be addressed.

complexes, proportional to the dipole magnitudes. Thioredoxin with an opposite dipole orientation shows no effect. Activating and inhibitory thioredoxin disulfides are distinguished by the charges of the residues 13/14 (α1 helix), 51 (α2–β3 linker), and 83/85 (β4–β5 linker), changing the dipole direction. The results show that the thioredoxin-target interplay may be controlled by the long-range interactions between the electrostatic dipole vectors of the proteins and the degree of their interface polarization.

Index Entries: 2-Oxoacid dehydrogenase complex; thioredoxin; protein–protein interaction; electrostatic dipole vector; structural homology.

Introduction

Recently we have shown that thioredoxin stimulates the 2-oxoacid dehydrogenase reactions, increasing the rate of catalysis and the substrate conversion degree *(1)*. Thioredoxins are small (approx 12 kDa) thermostable proteins with a conserved disulfide bridge in their active site *(2,3)*. Most of the biological effects of thioredoxins are dependent on their general thiol–disulfide oxidoreductase activity, providing the reversible oxidation/reduction of the dithiol/disulfide groups in target proteins. In particular, the residues essential for the thioredoxin thiol–disulfide reductase activity were shown to be required for its effect upon the 2-oxoacid dehydrogenase complexes *(1)*. The complexes catalyze the irreversible oxidation of 2-oxoacids yielding acyl-CoA's and NADH via Reactions 1–5:

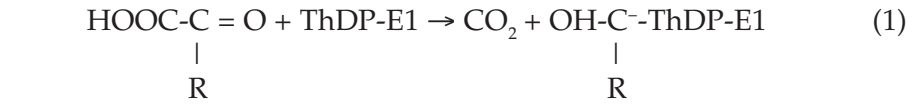

(1)

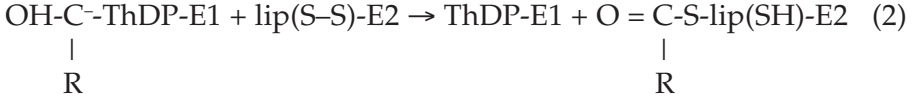

(2)

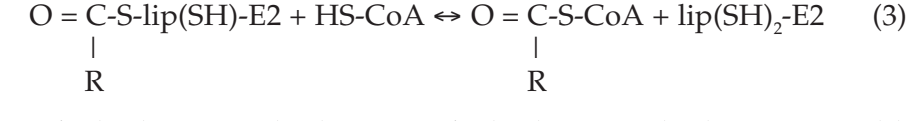

(3)

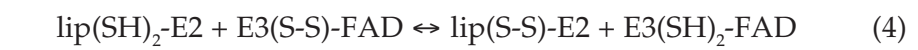

(4)

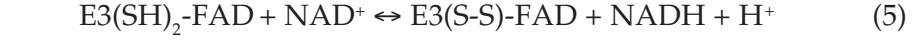

(5)

Two dithiol–disulfide couples are involved in the catalysis, with thioredoxin supposed to participate in the thiol–disulfide exchange with the complex-bound lipoate residue *(1)*. The thioredoxin-dependent activation of the complexes was revealed in the model system including mitochondrial dehydrogenases of 2-oxoacids and bacterial thioredoxin. To establish whether specific protein–protein interactions contribute to the interplay, cross-reactivity between a number of thioredoxins and 2-oxoacid dehydrogenase complexes is studied in this work. Sensitivity of the dehydrogenase complexes to the thioredoxin action is compared with the degree

of homology between the E3 components of the complexes and eukaryotic thioredoxin reductase, because the two enzymes belong to the same family of pyridine nucleotide-dependent disulfide oxidoreductases. The results point to the thioredoxin interaction with the E3 component of the complexes, related to the thioredoxin binding to thioredoxin reductase. The highest efficiency of the thioredoxin regulation is found in the system including both thioredoxin and 2-oxoacid dehydrogenase complex from mitochondria. Structural determinants for the specific action of mitochondrial thioredoxin are investigated by comparison of this protein to other thioredoxin species. Efficiency and specificity of different thioredoxins are correlated with features of their amino acid sequences and 3D structures analyzed by multiple sequence alignment and homology modeling. Interpretation of the biochemical effects on the structural level points to the polarization of the thioredoxin molecule and some spatial constraints as factors controlling the thioredoxin–target interplay. The degree of thioredoxin cross-reactivity with different proteins is shown to correlate with the polarization of its active site surroundings.

Materials and Methods

Materials

Coenzyme A, insulin, and DTNB were obtained from Sigma; ThDP, glutathione disulfide, and glutathione were from Serva; 2-oxoglutarate, pyruvate, cysteine, and cystine were from Merck; NAD^+ and DTT were from Boehringer; thioredoxin of *E. coli* was from Calbiochem.

Enzymes and Assays

2-Oxoglutarate and pyruvate dehydrogenase complexes were isolated from pig heart as in ref. *6*. Thioredoxin from pig heart mitochondria was isolated according to ref. *7*. The preparation of mitochondrial protein used in this work was characterized by the single band of 11.8 kDa in the sodium dodecyl sulfate-polyacrylamide gel electrophoresis (SDS-PAGE) under nonreducing conditions and a major peak in high performance capillary electrophoresis *(8)* and high-performance liquid chromatography (HPLC) (*see below*). The protein exhibited a high thioredoxin activity (4–7 ΔD_{650}/min/mg protein) in the insulin reduction test performed as in ref. *8*. Plant thioredoxins were a generous gift of Prof. Jacquot (Nancy, France). The concentration of thioredoxins was determined at 280 nm applying molar absorbance coefficients given by PROTPARAM of SWISSPROT database (http://expasy.hcuge.ch/sprot/protparam.html). The same tool was used to obtain the p*I* of different thioredoxins. The disulfide forms of thioredoxins were used.

Activities of 2-oxoglutarate and pyruvate dehydrogenase complexes were assayed as in ref. *1*. Kinetic measurements were carried out at 25°C on an *Uvicon* spectrophotometer (Kontron Instruments). Dispersion of the v_a/v

values given includes experimental errors in determination of both v_a and v according to the equation:

$$(v_a \pm \Delta v_a)/(v \pm \Delta v) = v_a/v \pm \sqrt{[(\Delta v_a/v)^2 + (v_a \cdot \Delta v/v^2)^2]}$$

N-Terminal Sequence Determination of Mitochondrial Thioredoxin

The samples to be analyzed were applied to HPLC under the standard conditions, using 0.1% trifluoroacetic acid in water as buffer A and 0.085% trifluoroacetic acid in acetonitrile as buffer B. HPLC was done on an ABI 173A MicroBlotter (PE Applied Biosystems) with on-line transfer of the eluent onto ProBlott membrane (PE Applied Biosystems). A column (Perkin Elmer C18, 0.5 × 150 mm) was equilibrated with 5% of buffer B for 30 min. After the sample injection, the protein was eluted in a 0.7-mL gradient from 5 to 45% of buffer B. The protein peak was sequenced on an ABI 494HT protein sequencer (PE Applied Biosystems) with standard cycles and automated sequence analysis.

Computer Modeling and Alignment

All modeling procedures were performed using the program SYBYL 6.3 *(9)* running on an IRIS Indy workstation. Homology modeling of rat mitochondrial thioredoxin was described in detail in ref. *10*. The 3D structures of thioredoxin from *E. coli* and thioredoxin *h* from *C. reinhardtii* were obtained from the Protein Data Bank Brookhaven *(11)*, entries 2TRX and 1TOF, respectively. Initial construction of the model structures of other thioredoxins were carried out using the Swiss-Model Automated Protein Modeling service. Full geometry optimization was performed with the program AMBER 4.0 *(12)* running on a CONVEX-220 using the Kollman all atom force field *(13)*. The structures were solvated in a shell of TIP3P-water *(14)* and geometry was optimized by 5000 step conjugate gradient energy minimization. Electrostatics potential surfaces and dipole vectors were computed with the program GRASP *(15)*. The calculated dipole vectors were visualized with the SYBYL program package. All amino acids were considered to have standard protonation states at pH 7.0. Sequence alignment was computed using the program CLUSTALW, available at the Internet Server of the Baylor College of Medicine (BCM) and visualized with the program GeneDoc (*16*).

Results

Thioredoxin effects on the pyruvate and 2-oxoglutarate dehydrogenase complexes from mammalian and bacterial sources are shown in Fig. 1. Different concentrations of the *E. coli* and mitochondrial thioredoxins had to be applied to get the same effects. In all cases bacterial thioredoxin was less efficient than the mitochondrial one, in spite of their similar activities in a nonspecific insulin-reduction test. The sensitivity of the distinct complexes to a thioredoxin also differs. At fixed NAD^+ and thioredoxin

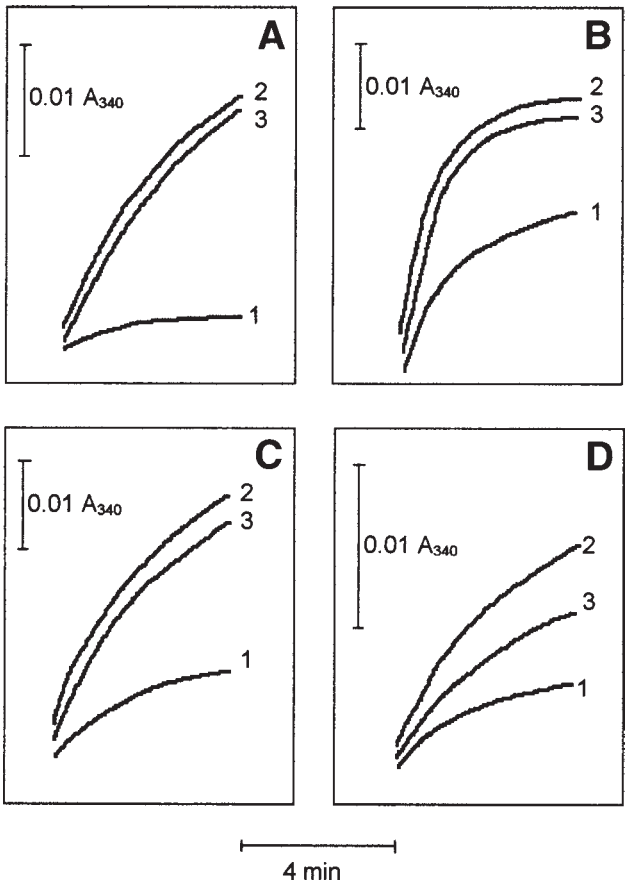

Fig. 1. Product accumulation curves of mammalian **(A,C)** and bacterial **(B,D)** 2-oxoacid dehydrogenase complexes at saturating concentrations of 2-oxoacid and CoA and low NAD^+. 1, the control; 2, in the presence of thioredoxin from pig heart mitochondria; and 3, in the presence of *E. coli* thioredoxin. **(A)** Pig heart 2-oxoglutarate dehydrogenase complex (0.003 mg/mL); 5 μ*M* NAD^+; 0.5 μ*M* mitochondrial thioredoxin; 1 μ*M* thioredoxin of *E. coli*. (**B**) *Azotobacter vinelandii* 2-oxoglutarate dehydrogenase complex (0.008 mg/mL); 16 μ*M* NAD^+; 0.5 μ*M* mitochondrial thioredoxin; 1.6 μ*M* thioredoxin of *E. coli*. (**C**) Pig heart pyruvate dehydrogenase complex (0.014 mg/mL); 8 μ*M* NAD^+; 0.5 μ*M* mitochondrial thioredoxin; 3 μ*M* thioredoxin of *E. coli*. (**D**) *E. coli* pyruvate dehydrogenase complex (0.005 mg/mL); 16 μ*M* NAD^+; 2 μ*M* mitochondrial thioredoxin; 6.8 μ*M* thioredoxin of *E. coli*.

concentrations, stimulation of the 2-oxoglutarate and pyruvate dehydrogenase complexes from mitochondria is higher than that of the *Azotobacter vinelandii* and *E. coli* systems (Table 1). The latter represents the least influenced complex, whose activity is increased only at relatively high thioredoxin concentrations and prolonged reaction time (Fig. 1D) even in the presence of thioredoxin from the same source. The sensitivity of the complexes to thioredoxin correlated with the degree of homology between their dihydrolipoamide dehydrogenase components (E3) and eukaryotic thioredoxin reductase. The two enzymes belong to the same family of pyridine

Table 1
Activation of Different 2-Oxoacid Dehydrogenase Complexes by Mitochondrial Thioredoxin[a]

2-Oxoacid dehydrogenase complex	Concentration, mg/mL	v_a/v, %
2-Oxoglutarate dehydrogenase pig heart	0.003	650 ± 50
2-Oxoglutarate dehydrogenase *A. vinelandii*	0.003	280 ± 25
Pyruvate dehydrogenase pig heart	0.014	190 ± 25
Pyruvate dehydrogenase *E. coli*	0.005	100 ± 15

[a]The ratio of the initial velocity with 0.5 μ*M* thioredoxin to that without thioredoxin (v_a/v, %) is given. Activity was measured at 8 μ*M* NAD^+.

nucleotide-dependent disulfide oxidoreductases, suggesting the E3 component of the complexes to be involved in the thioredoxin binding. The alignment of the sequences *(17–20)* (Fig. 2) showed an increase in the homology degree from the *E. coli* to *A. vinelandii* and mammalian E3 components (41, 45, and 47% of conservative amino acid residues, respectively; Table 2), correspondent to an increase in the thioredoxin effect (Table 1). These data suggest that the complexes may bind thioredoxin in a way related to that in thioredoxin reductase.

The thioredoxin activation is revealed when the 2-oxoacid dehydrogenase reaction is measured with high concentrations of 2-oxoacid, CoA, and low NAD^+ *(1)*. In this case the reaction rates in the absence of thioredoxin decrease with the reaction time (Fig. 1). Preincubation of the complexes with the components of reaction mixture demonstrated that neither 2-oxoacid nor CoA alone induced such inactivation, but their combination caused the loss in V_{max}. The inactivation is prevented by thioredoxin (Table 3). Thus, thioredoxin effects on the 2-oxoacid dehydrogenases can be measured in two sets of experiments. First, thioredoxins induce an increase in the initial reaction rate of the 2-oxoacid oxidation at low NAD^+ concentrations (Fig. 1 and Table 1). Second, thioredoxins protect from the V_{max} decrease on preincubation of the complexes with 2-oxoacid and CoA (Table 3).

Table 4 demonstrates the thioredoxin effects on the reaction rates at low NAD^+. It is obvious that thioredoxin from mitochondria was an order of magnitude more efficient than those from *E. coli*, pea *m*, and *Clamydomonas reinhardtii h*. Thioredoxin *f* from pea was inactive, whereas *m* from *C. reinhardtii* caused an inhibition. The $S_{0.5}$ value of the latter was close to those of *E. coli* and pea *m* proteins, suggesting similar binding affinity in spite of the opposite effect (inhibition instead of activation). A small amplitude of the response was inherent in *Arabidopsis thaliana* thioredoxins. For instance, *h5* protein elicited approx 30% of maximum activation observed with other species shown in Table 4.

Fig. 2. Multiple sequence alignment of human thioredoxin reductase with the dihydrolipoamide dehydrogenase components of the complexes studied in this work. *E. coli* E3 numbering is given at the top. The particular domains of the enzymes are

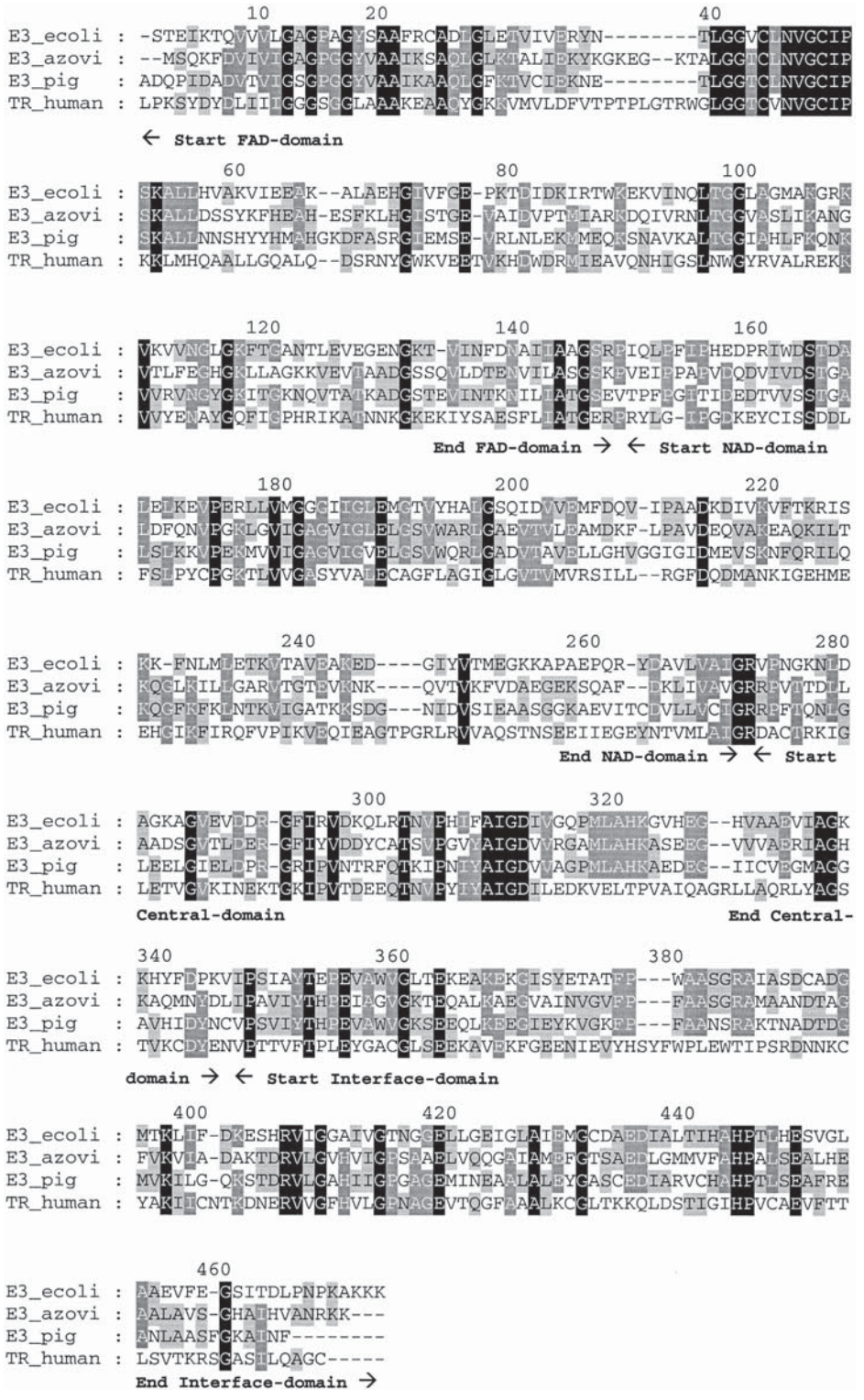

Fig. 2. *(continued)* indicated below the sequences. Residues are shaded in different intensities according to the degree of their conservation in different sequences. The target sequence of mitochondrial E3 (from pig heart) is excluded from consideration.

Table 2
Conservation Between Sequences of Dihydrolipoamide Dehydrogenase (E3) from Different Species and Human Thioredoxin Reductase[a]

	E3 ecoli	E3 azovi	E3 pig	TR human
	1	2	3	4
	473	38%	40%	2%
1	0	59%	57%	41%
	0	2%	3%	6%
	187	477	47%	23%
2	287	0	65%	45%
	14	0	3%	4%
	193	231	474	26%
3	279	316	0	47%
	17	19	0	5%
	114	116	131	491
4	207	224	234	0
	32	24	27	0
	1	2	3	4

[a]E3's from *E. coli* (1), *A. vinelandii* (2), pig heart (3), and human thioredoxin reductase (4) are compared pairwise and characterized by three distinct values computed with CLUSTALX, which are expressed in percentages (above the main diagonal) and in number of amino acids (below the main diagonal). The first value corresponds to identical amino acids, the second one equals the identical and structurally homologous amino acids, and the third value gives the gaps between the sequences.

Table 3
Inactivation of 2-Oxoacid Dehydrogenase Complexes by Preincubation with 2-Oxoacids and CoA and its Alleviation by *E. coli* Thioredoxin[a]

2-Oxoacid dehydrogenase complex	Concentration, mg/mL	Preincubation time (min)	Thioredoxin, (3.5 μ*M*)	Inactivation $1 - v_a/v$ (%)
2-Oxoglutarate dehydrogenase *A. vinelandii*	0.008	4	–	80
			+	40
2-Oxoglutarate dehydrogenase pig heart	0.009	4	–	50
			+	0
Pyruvate dehydrogenase *E. coli*	0.002	10	–	75
			+	40

[a]The complexes were preincubated with saturating concentrations of the two substrates in the reaction medium without NAD^+. The initial rate of the reactions started by addition of 2.5 m*M* NAD^+ was measured.

Table 4
Effect of Different Thioredoxins
on Pyruvate and 2-Oxoglutarate Oxidation[a]

Thioredoxin	Effect	$S_{0.5}$ (μ*M*) 2-Oxoglutarate dehydrogenase complex	$S_{0.5}$ (μ*M*) Pyruvate dehydrogenase complex
Mitochondrial	Activation	< 0.25	< 0.1
E. coli	Activation	1 ± 0.5	1 ± 0.2
m pea	Activation	1 ± 0.4	1.5 ± 0.5
h C. reinhardtii	Activation	5 ± 2	4 ± 1
h5 A. thaliana	Low activation	15 ± 5	Not determined
f pea	None	—	—
m C. reinhardtii	Inhibition	1 ± 0.5	Not determined

[a]The initial activity of corresponding complexes was measured in the medium with saturating concentrations of 2-oxoacid and CoA and 5 or 30 μ*M* NAD^+ in the case of activation or inhibition, respectively.

Similar differences in the thioredoxin efficiencies were revealed from the thioredoxin protection of the complexes inactivated by 2-oxoacid and CoA. The residual activity was already increased at extremely low (0.05 μ*M*) concentration of mitochondrial thioredoxin and the protection was complete at 0.5 μ*M*, whereas other species did not exhibit a significant effect within this concentration range (Table 5). The *E. coli*, pea *m*, and *C. reinhardtii h* thioredoxins provided full protection at concentrations 3–5 μ*M*. Three of the five known thioredoxins *h* from *A. thaliana* were only partially protective, decreasing the inactivation from 70 to 30% (*h4*,*h5*) or to 50% (*h1*). The further increase in the thioredoxin concentrations gave no additional protection. The low protection correlated with the partial (in comparison to other species) activation by *A. thaliana h5* protein (Table 4). Thioredoxins that were not activating (*A. thaliana h2, h3,* pea *f*, *C. reinhardtii m*) were not effective in the protection either. Thus, on the basis of two independent sets of data thioredoxins could be ordered according to their ability to influence 2-oxoacid dehydrogenase complexes as shown in Tables 4 and 5.

Multiple sequence alignment was performed using the known structures of thioredoxins employed *(21–27)*, with numbering the *E. coli* thioredoxin residues applied to all the species used (Fig. 3). The four sequences of mammalian mitochondrial thioredoxins, i.e., rat, mouse, ox, and human, available from the database SWISSPROT possess 96–100% identity with no more than four substitutions (V6I, M47V, I68L, I81M) as compared to the sequence of rat mitochondrial thioredoxin presented in Fig. 3. Sequencing of the pig heart mitochondrial protein used in this work resulted in the following N-terminus: TTFNIQDGPDFQDRVVNSETP VVVDFHAQ. These 29 N-terminal residues are identical to those of the bovine and human species and contain the only substitution, I6V, com-

Table 5
Protection of the Pig Heart 2-Oxoglutarate Dehydrogenase Complex from the 2-Oxoglutarate and CoA-Induced Inactivation by Different Thioredoxins[a]

	v_a/v (%) at thioredoxin concentration (μ*M*)							
Thioredoxin	0	0.05	0.5	3	5	10	20	80
None	30 ± 10							
Mitochondrial		59 ± 5	100 ± 8					
E. coli			32 ± 10	100 ± 12				
m pea			22 ± 10		100 ± 4			
h C. reinhardtii			23± 10	60 ± 7	100 ± 3			
h4 A. thaliana		22 ± 10	51 ± 7	68 ± 8		66 ± 8		
h5 A. thaliana			32 ± 10				60 ± 5	70 ± 5
h1 A. thaliana		33 ± 10		52 ± 15		51 ± 15		
f pea			33 ± 10		41 ± 12	41 ± 10		
h2 A. thaliana		22 ± 10		25 ± 14		30 ± 14		
h3 A. thaliana			43 ± 10				31 ± 15	11 ± 10
m C. reinhardtii		40 ± 10	30 ± 10	17 ± 14	19 ± 10			

[a]Conditions see Table 3.

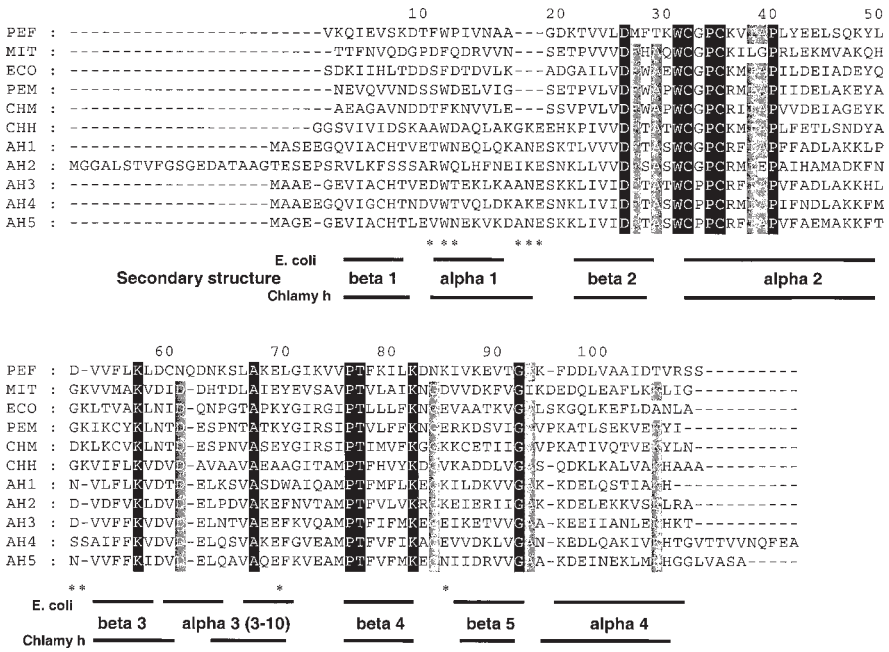

Fig. 3. Multiple sequence alignment of the thioredoxins used. Numbering of the *E. coli* thioredoxin residues is given at the top. Residues are shaded in different intensities as in Fig. 2. The residues discussed are marked at the bottom by asterisks. The secondary structure elements of thioredoxins from *E. coli* and *C. reinhardtii h* are presented below the alignment.

pared to rat and mouse proteins. Such conservation of the mitochondrial protein structure is remarkable, since it is not a general property of the same thioredoxin type. For instance, thioredoxin *m* from higher plants shows many more substitutions (*2*, Fig. 2). This indicates that highly conservative amino acid sequence of the mitochondrial thioredoxin may code some properties essential for its functioning. As will be shown below, this sequence provides exceptionally high separation of the charged residues on the molecule surface in comparison to eight other thioredoxins analyzed. This unique feature, which seems to be functionally important, is in accord with the decreased variety of the mitochondrial thioredoxin sequence, since such a strong positioning of the charged residues within the given 3D structure of thioredoxins must restrict the number of possible variations.

An obvious structural difference of the low or not effective thioredoxins *h* is elongation of the α1 helix owing to the three-residue insertion between the 19th and 20th amino acid of *E. coli* thioredoxin. In most cases it is accompanied by shortening the turn between the α2 helix and β3 strand due to the absence of K52 (Fig. 2, *2*). Noteworthy, K52 is present in all thioredoxins, including the only thioredoxin of *h* type (from *C. reinhardtii)*, which elicit a 100% amplitude of activation. In contrast, the α2–β3 linker

does not contain the lysine residue in thioredoxins exhibiting a low (*A. thaliana h1*, *h4*, *h5)* or no (*A. thaliana h3*, *h2*, pea *f*) effect. Thus, the length of the α1 helix and the positive charge of K52 in the α2–β3 linker correlate with the amplitude of thioredoxin action on the 2-oxoacid dehydrogenase complexes. Other factors contributing to the low or no effects observed may include the active site sequence CPPC in *h3*, *h4*, and *h5* thioredoxins instead of the regular one, CGPC, in other species and a longer N-terminus of *h2* thioredoxin (Fig. 3). The latter presumably comprises a target sequence and the nonmature proteins are known to be inactive.

Figure 3 also shows that all effective thioredoxins have Y70, which is not present in the species eliciting low or no effect. According to the resolved structures of thioredoxins *(28–30)*, Y70 interacts through van der Waals contacts with the phenylalanine residue in the α1 helix of the thioredoxin molecule (F12 in *E. coli* thioredoxin). Noteworthy that the *A. thaliana* thioredoxins form this couple by more bulky and hydrophobic residues (W12W70 or W12F70, Fig. 2) than those present in the reactive thioredoxins. Hence, not only the length of the α1 helix, but also its interaction with the $\alpha 3/3_{10}$ helix seems to be important.

The inhibitory action of *C. reinhardtii* thioredoxin *m* (Table 4) was remarkable. Since it was not inherent in the homologous pea *m* protein, the structural determinants of this inhibition were studied by comparison of the similar sequences of both *m* type thioredoxins used. With most of amino acid residues conserved and many substitutions being functionally equivalent (like S to T, V to I, etc.), only a limited number of potentially significant functional groups were found to differ. After checking the corresponding positions in other activating thioredoxins, the systematic features distinguishing the inhibitory (*C. reinhardtii* thioredoxin *m)* and activating (mitochondrial, *E. coli*, pea *m*, and *C. reinhardtii h*) species were revealed (Fig. 3). First, all activating thioredoxins possess a negative charge (D13 or D14) next to the previously discussed F/W12 residue, whereas the positive charge at this position (K13) is specific for the inhibitory thioredoxin. Second, the uncharged glycine residue precedes K52 in the α2–β3 linker of the activatory species, but it is replaced by the negatively charged aspartate residue in the inhibitory thioredoxin. Third, the β4–β5 linker has the negatively charged D/E85 or D83 in activatory thioredoxins and the positively charged K85 in the inhibitory one. All these residues are located on the thioredoxin surface opposite to the catalytic site. Thus, our findings show that the remote from the active center electrostatic charges may influence the thioredoxin reactivity to the 2-oxoacid dehydrogenase complexes.

The available X-ray data, in particular, those for the proteins from *E. coli (28)* and *C. reinhardtii h (30)*, the known sequences of other species *(21–27)*, and similar tertiary structure of all thioredoxins allowed us to apply homology modeling *(10)* to the proteins with the 3D structures yet unresolved. The 3D models created reveal a remarkable difference in the distribution of the electrostatic charges on the protein surface. Figures 4 and 5 present its part including the active site disulfide. This part of the molecule

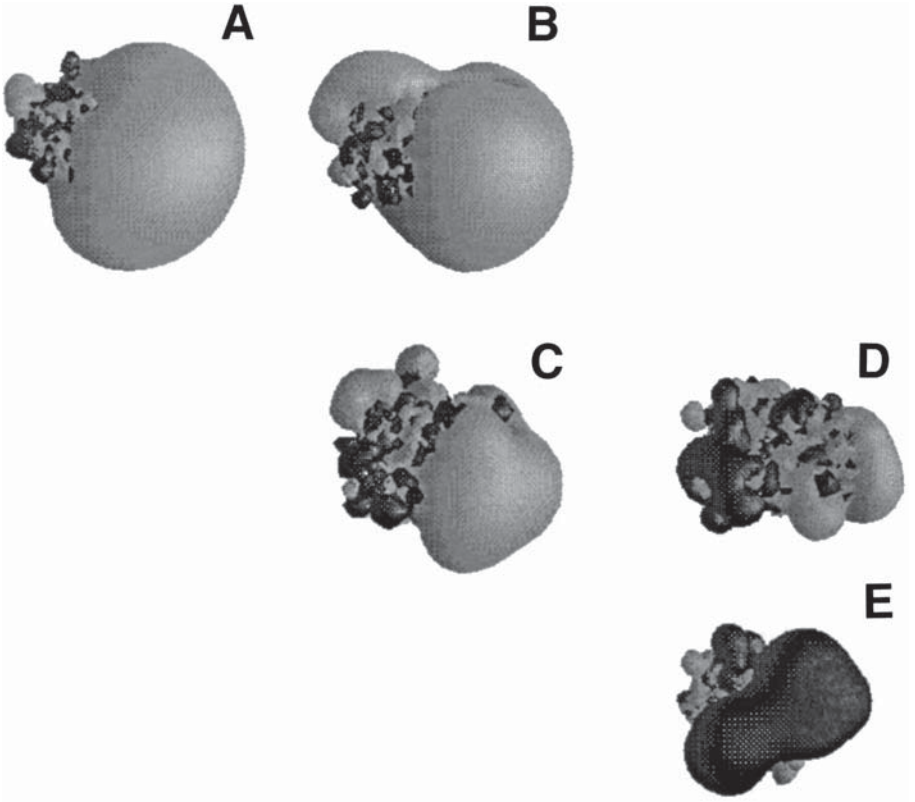

Fig. 4. Electrostatic potential plot produced with the program GRASP for the thioredoxin proteins: of rat mitochondria **(A)**, *h3* of *A. thaliana* **(B)**, *h5* of *A. thaliana* **(C)**, *h1* of *A. thaliana* **(D)**, and pea *f* **(E)**. Isopotential lobes are shown for –2 kt (grey) and +1 kt (black). The view-axis points to the active site disulfide and surroundings.

is seen to interact with the target in the cocrystallized binary complex of the target peptide with human thioredoxin *(31)*. Figure 4 exhibits the diversity in the electrostatic features of this area in different thioredoxin species. There are mostly negative (A,B), positive (E), and intermediary (C,D) surfaces. The data on thioredoxin action show that the extreme cases (Fig. 4A,B,E) imply more specificity to a target than those intermediary (C,D). Indeed, both pea *f* and *h3* thioredoxins do not react with the 2-oxoacid dehydrogenase complexes, which are not their targets. On the other hand, mitochondrial thioredoxin is highly efficient against these mitochondrial systems (Tables 4 and 5), but is not reactive toward other thioredoxin-regulated enzymes *(5)*. Unlike the thioredoxins with highly polarized surface near the active site (Fig. 4A,B,E), all the species exhibiting a nonspecific reactivity to the 2-oxoacid dehydrogenase complexes are characterized by the intermediary charge distribution in this area (Fig. 5). In particular, when the structurally similar *h1*, *h3*, and *h5* thioredoxins are compared, the cross-reactivity is apparent with *h1* and *h5* species, but not with *h3* one (Table 5). This is in good accord with the fact that *h1* and *h5* thioredoxins

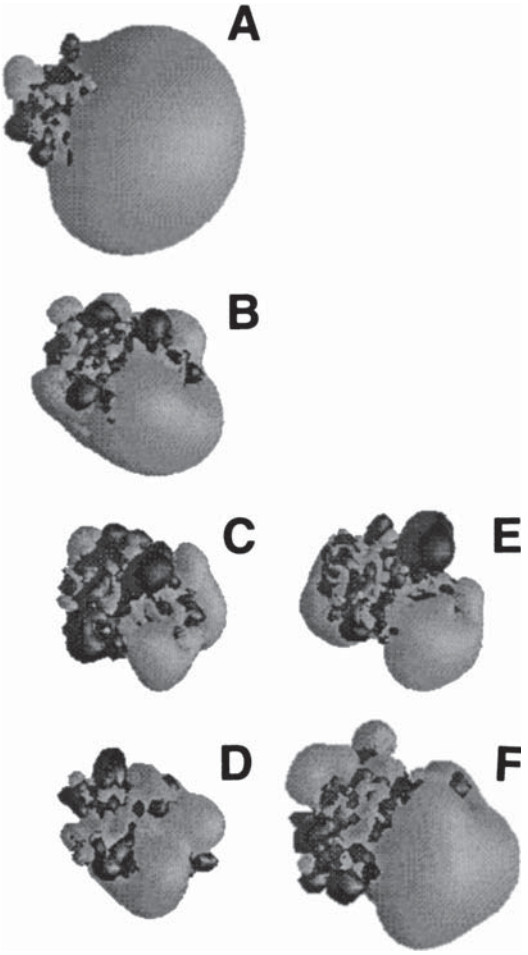

Fig. 5. Electrostatic potential plot produced with the program GRASP for the thioredoxin proteins: of rat mitochondria **(A)**; *E. coli* **(B)**; *m* of pea **(C)**; *h* of *C. reinhardtii* **(D)**; *m* of *C. reinhardtii* **(E)**; and *h5* of *A. thaliana* **(F)**. Isopotential lobes and view-axis as in Fig. 4.

(Fig. 4C,D) have not so tightly localized charges as the *h3* protein (Fig. 4B). A lower efficiency of *h3* protein compared to *h1* and *h5* species was revealed also with the sorghum $NADP^+$-malate dehydrogenase *(21)*. Thus, the intermediary polarization of the potential interface (Fig. 5) results in a better cross-reactivity, while an increased separation of the charges in this region (Fig. 4A,B,E) restricts nonspecific interactions. This result is consistent with the induced-fit model and multiple binding points on the protein–protein interactions. When thioredoxin interacts with a protein, there are more chances to meet a complementary charge, if the interacting surfaces possess the intermediary charge distribution (Fig. 5). Even if the specific residue designed for this interaction is absent, a neighboring one may happen to substitute for that specific residue. Contrary to that, with the tightly local-

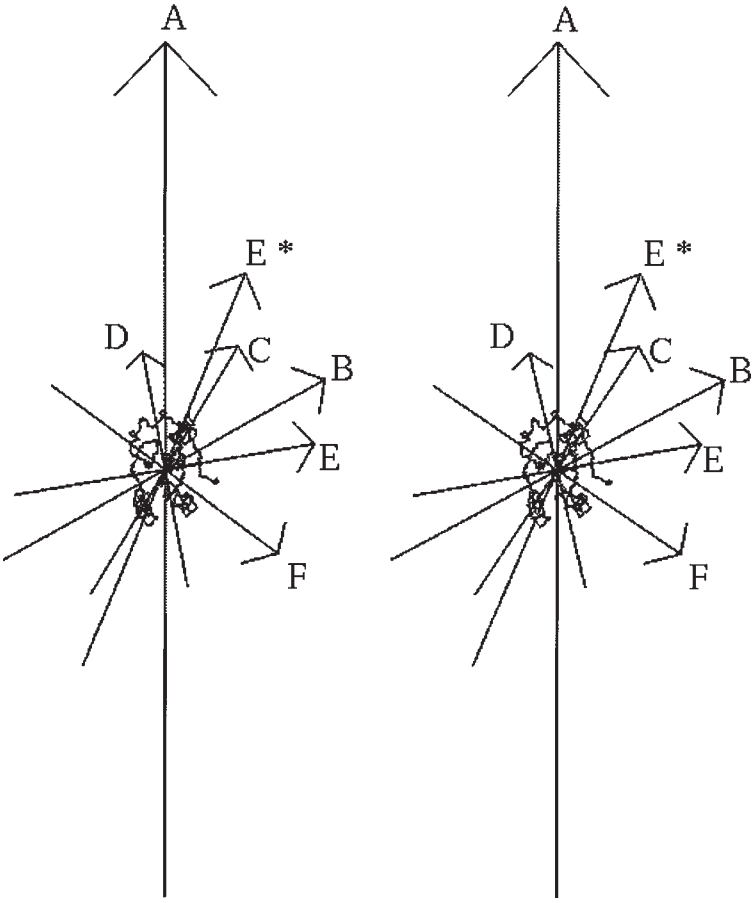

Fig. 6. Stereo view of the dipole vectors of the superpositioned structures of rat mitochondrial **(A)**, *E. coli* **(B)**, pea *m* **(C)**, *C. reinhardtii h* **(D)**, *C. reinhardtii m* **(E)**, and pea *f* **(F)** thioredoxins. The dipole vector of *C. reinhardtii m* thioredoxin with the substituted residues (*see text*) is marked by asterisk (E*).

ized charges (Fig. 4A,B,E), their specific positions assume greater importance. In this case the probability of substitution by a neighboring group is low, and the binding is therefore much more dependent on the presence of the specific residue.

A high degree of charge separation causing the molecule polarization is observed not only in the active site surroundings of mitochondrial thioredoxin (Fig. 4A), but also in other projections of this molecule. This results in the highest electrostatic dipole value of the protein (Fig. 6 and Table 6). It is remarkable that the dipole vectors inherent in thioredoxins, which activate/protect, have a similar direction (angle difference less than 90°). Moreover, in this case the thioredoxin efficiencies ($S_{0.5}$; Table 4) are proportional to the total dipole values (Table 6), with both parameters forming the same row (first five lines in the Tables 4 and 6). The pea *f* thioredoxin has no effect and does not seem to bind to the 2-oxoacid dehydrogenase

Table 6
Physico-Chemical Parameters of Thioredoxins Used

Thioredoxin	p*I*	Molecule net charge	Total dipole value, Db
Mitochondrial	4.9	–6	580
E. coli	4.7	–5	288
Pea *m*	5.4	–2	281
h C. reinhardtii	5.9	–2	227
A. thaliana h5	5.2	–4	227
A. thaliana h3	5.1	–6	267
A. thaliana h1	5.6	–2	333
Pea *f*	8.2	+1	319
m C. reinhardtii	5.1	–2	244

complexes so far. This is in good accord with the reversed polarization of its active site surroundings (Fig. 4E) and an opposite direction of its dipole vector compared to that of mitochondrial thioredoxin (Fig. 6). The dipole vector inherent in inhibitory *C. reinhardtii m* thioredoxin is almost orthogonal to the mitochondrial thioredoxin dipole (Fig. 6). Noteworthy that after substitution of the residues distinguishing the inhibitory thioredoxin *m* (K13, D51, K85) by those present in activating thioredoxins (D13, G51, E85), the dipole of *C. reinhardtii m* thioredoxin significantly changes its direction, approximating that in activating species (Fig. 6, vector with asterisk). Thus, the "inhibitory" residues may influence the thioredoxin action by change in the dipole direction.

The *A. thaliana h1*, *h3*, and *h5* thioredoxins are characterized by dipole vectors similar to the activating thioredoxins in both orientation (not shown) and magnitude (Table 6). In spite of the low amplitude of the effects elicited by *A. thaliana* thioredoxins (Tables 4 and 5), saturation of the *h1* effect is achieved already at 3 μ*M* (Table 5), pointing to the $S_{0.5}$ as in other effective species. The $S_{0.5}$ of *h5* protein is close to that of *C. reinhardtii h* thioredoxin (Table 4). Thus, compared to other thioredoxins, *h1* and *h5* species have the affinities to the complexes in accordance with their dipole orientation and magnitudes. However, the properly oriented dipole vector of *h3* thioredoxin cannot help its interaction with the complexes, since the tightly localized charges in the binding area (Fig. 4B) do not support this interaction, as pointed above. Obviously, the dipole vector affects the affinity only on the eligible electrostatics of the active site surroundings (Fig. 5), which is needed for the complex formation.

Thus, with other conditions being equal, the thioredoxin function is shown to depend on the charge separation in the active site surroundings and orientation and magnitude of the electrostatic dipole vector of the whole thioredoxin molecule. The correlation of these electrostatic properties with the thioredoxin efficiency (Tables 4 and 5) is much better than that observed between the efficiency and the thioredoxin p*I* or net charge (Table 6).

Discussion

A study of enzyme interaction with a ligand and its structural analogs represents a well-known enzymological approach to characterize a binding process. In this work, this approach was used to study protein–protein interactions using a computer-generated comparison of protein structures. A number of homologous thioredoxins were tested as ligands of different 2-oxoacid dehydrogenase complexes. The highest regulatory potential has been found in the mitochondrial couple. This result supports the physiological relevance of the interplay between the 2-oxoacid dehydrogenase complexes and mitochondrial thioredoxin, pointing to specific protein–protein interactions involved.

Differences in the thioredoxin efficiencies (Table 4) manifest the essential role of the thioredoxin structure in its interaction with the 2-oxoacid dehydrogenase complexes. Similar row of preference to different thioredoxins exhibited by both pyruvate and 2-oxoglutarate dehydrogenase systems (Table 4) suggests that the common component of these multienzyme systems, E3, interacts with the effector. The correlation found between the sensitivity of the corresponding complexes to the thioredoxin action (Table 1) and the E3-thioredoxin reductase homology (Table 2) is in good accord with this assumption. Besides, it indicates that thioredoxin may bind to the E3 component in a way related to that in the thioredoxin reductase–thioredoxin complex. These findings agree with the kinetic data about the dependence of the thioredoxin effects on the E3-catalyzed dihydrolipoate oxidation *(1)*. Thioredoxin "anchoring" on E3 may be envisaged like in Fig. 7. Because the action of thioredoxin appears to be influenced by the structural elements remote from the catalytic center (i.e., the α1 helix, charges in the α2–β3 and β4–β5 linkers), the thioredoxin "back" may be suggested to interact with E3, whereas the opposite site with the active site disulfide is available to the complex-bound lipoate (Fig. 7). The catalytically important areas of the 2-oxoacid dehydrogenase complexes appear to be involved in the thioredoxin binding. This is supported by the inhibition of 2-oxoacid oxidation, observed in the presence of *C. reinhardtii* thioredoxin *m* (Table 4) or the catalytically inactive *E. coli* thioredoxin *(1)*. In particular, the inhibitory action of the modified *E. coli* thioredoxin shows that the binding that is not accompanied by thiol–disulfide exchange is inhibitory. Hence, the reversed charges in the "anchoring" area of the *C. reinhardtii m* thioredoxin may result in the inhibition owing to improper orientation of the catalytic groups and/or steric blockade of the E3 active site in the complex formed with this thioredoxin (Fig. 7, dotted line).

Our data show that the thioredoxin binding depends on polarization of both the whole thioredoxin molecule and its part facing the target. The former is known to regulate the long-range interactions between the proteins through mutual orientation of their electrostatic dipole vectors *(32)*, whereas the latter is obviously important for the short-range interactions stabilizing the thioredoxin–target complex. A significant role of electro-

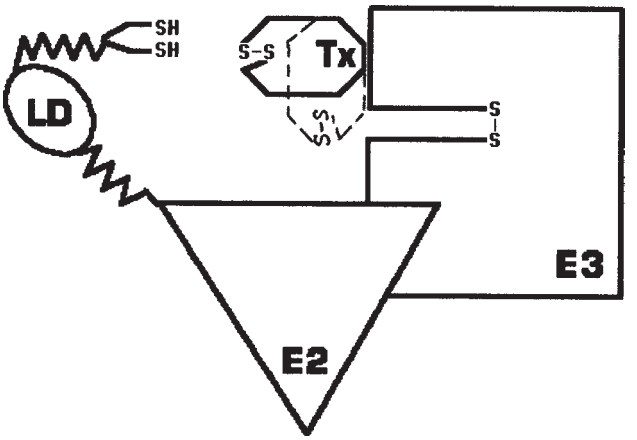

Fig. 7. Hypothetical scheme of the thioredoxin interaction with 2-oxoacid dehydrogenase complexes. LD, lipoyl domain; Tx, thioredoxin. Inhibitory mode of thioredoxin interaction is shown by the dotted line.

static dipoles of macromolecules in their proper docking into binding sites was noted in the studies on receptor binding of growth factors *(33)* and ferredoxin binding to ferredoxin reductase *(34)*. Theoretical estimations *(32)* indicate that polarization of interacting surfaces brings about the advantage of their correct preorientation determined by the electrostatic dipole vectors already at long-range distances. Proper alignment of dipoles increases the probability of successful collisions, i.e., the collisions that favor stabilization of the complex by the corresponding short-range interactions. The increased number of such collisions is equivalent to a decrease in effective concentrations of interacting proteins. This is in accord with the ability of the thioredoxin with the highest dipole magnitude (the mitochondrial protein) to work at the lowest concentrations (down to 10^{-7} *M*; Table 1). However, the proper direction and magnitude of dipoles do not ensure the complex formation unless the corresponding short-range interactions are realized. The latter is defined by a specific electrostatic pattern of the thioredoxin active site surroundings (Figs. 4 and 5). Our data show that the relative specificity of a thioredoxin may be predicted from this electrostatic pattern, with more polarization implying more specificity. This finding could be used to work out a "functional" classification of thioredoxins, in addition to the phylogenetic analysis of thioredoxin structures, currently used for their comparison *(2,3,21)*. At the moment, many thioredoxins have been characterized by genome screening, without knowledge of their biological function. We show in this work that the modeling of thioredoxin 3D structures, followed by analysis of the molecule electrostatic properties, may indicate the potential specificity of a thioredoxin, helpful in searches for the corresponding target system.

Correct electrostatic properties do not compensate other structural constraints. In fact, *h1* and *h5 A. thaliana* thioredoxins have eligible bind-

ing surfaces and proper electrostatic dipole vector that provides reasonable affinities for the complexes. However, their effects are of low amplitude (Tables 4 and 5), which obviously reflects the catalytic incompetence of these thioredoxins in the thiol–disulfide exchange with the complex-bound lipoate residue. This may be related to the absence of K52, the increased length of the α1 helix and the different contact of the latter with the $\alpha 3/3_{10}$ helix through the residues 12 and 70. Because the $\alpha 3/3_{10}$ helix belongs to the potential target interface presented in Figs. 4 and 5, changes in the α1 helix may influence the geometry of this catalytically important area through the interaction between the helices. Role of this interaction in the thioredoxin function is supported by the fact that in human thioredoxin Y70 is substituted by one of the additional cysteine residues (*see* multiple alignment in ref. 2) involved in the redox regulation of this protein *(35)*.

The electrostatic and spatial differences may represent two ways of adjusting to a target on the level of the thioredoxin integral structure. Molecules with improper electrostatics do not interact. Those with proper electrostatics do, but their complex may be catalytically inactive owing to steric factors. Only in the case of both electrostatics and geometry being correct is the catalytically competent thioredoxin–target complex efficiently formed. Obviously, this control is especially important when several thioredoxins are supposed to specifically influence their target enzymes within the same cellular compartment.

Given the identical mechanism of the thioredoxin-catalyzed thiol–disulfide oxidoreduction, provided by the conserved structures of the thioredoxin active sites and surroundings, selective action of thioredoxin should stem from specific recognition on formation of the thioredoxin–target complex. If the recognizing and catalytic groups comprise the same area, the high reactivity of the essential cysteine residues makes the control of oxidoreduction between dithiol–disulfide couples in thioredoxin and target difficult. In this case the significance of long-range interactions should be increased, since they allow the recognition process to be started before the highly reactive catalytic groups are brought together. The correlation found between the electrostatic dipole vectors and efficiencies of different thioredoxins argues for the long-range electrostatic interactions to be of special significance in the thioredoxin-target recognition. The spatial separation of the recognizing and catalytic groups as shown in Fig. 7 represents an additional way to regulate the thioredoxin selectivity, which may be realized on thioredoxin interaction with biological structures of extended dimensions.

Acknowledgments

This work was supported by Alexander von Humboldt Foundation (Germany). We are indebted to Prof. J.-P. Jacquot (Nancy, France) for the plant thioredoxin samples.

References

1. Bunik, V., Follmann, H., and Bisswanger, H. (1997), *Biol. Chem.* **378,** 1125–1130.
2. Jacquot, J.-P., Lancelin, J.-M., and Meyer, Y. (1997), *New Phytol.* **136,** 543-570.
3. Follmann, H. and Haeberlein, I. (1995/1996), *Biofactors* **6,** 147–156.
4. Berg, A. and de Kok, A. (1997), *Biol. Chem.* **378,** 617–634.
5. Bodenstein-Lang, J., Buch, A., and Follmann, H. (1989) *FEBS Lett.* **258,** 22–26.
6. Bunik, V. I. and Follmann, H. (1993) *FEBS Lett.* **336,** 197–200.
7. Bunik, V., Shoubnikova, A., Bisswanger, H., and Follmann, H. (1997), *Electrophoresis* **18,** 762–766.
8. Holmgren, A. (1979), *J. Biol. Chem.* **254,** 9627–9632.
9. TRIPOS Associates (1994), Molecular Modeling Program 6.0 St. Louis, MO, Tripos Associates.
10. Raddatz, G., Bunik, V. I., Scior, T., and Bisswanger, H. (1997), *J. Mol. Model.* **3,** 359–363.
11. Bernstein, F. C. and Tasumi, M. (1977), *J. Mol. Biol.* **112,** 535–540.
12. Kollman, P. A. and Weiner, S. J. (1991), *J. Comp. Chem.* **2,** 287–299.
13. Weiner, S. J., Kollman, P. A., Case, D. A., Singh, U. C., Ghio, C., Alagona, G., Profeta, S., and Weiner, P. (1984), *J. Am. Chem. Soc.* **106,** 765–780.
14. Jorgensen, W. L., Chandrasekhar, J., Madura, J., Impey, R., and Klein, M. (1983), *J. Chem. Phys.* **79,** 926–931.
15. Honig B. and Nicholls A. (1995), *Science* **268,** 1144–1149.
16. Nicholas, K. B. and Nicholas, H. B. Jr., (1997), GeneDoc: a tool for editing and annotating multiple sequence alignments. Distributed by the author (http://www.cris.com/~ketchup/genedoc.shtml).
17. Westphal, A. H. and DeKok, A. (1990), *Eur. J. Biochem.* **187,** 235–239.
18. Stephens, P. E., Lewis, H. M., Darlison, M. G., and Guest, J. R. (1983), *Eur. J. Biochem.* **135,** 519–527.
19. Otulakowski G. and Robinson B. H. (1987), *J. Biol. Chem.* **262,** 17,313–17,318.
20. Gasdaska, P. Y., Gasdaska, J. R., Cochran, S., and Powis, G. (1995), *FEBS Lett.* **373,** 5–9.
21. Rivera-Madrid, R., Mestres, D., Marinho, P., Jacquot, J.-P., Decottignies, P., Miginiac-Maslow, M., and Meyer, Y (1995), *Proc. Natl. Acad. Sci. USA* **92,** 5620–5624.
22. Holmgren A. (1968), *Eur. J. Biochem.* **6,** 475–484.
23. Spyrou, G., Enmark, E., Miranda-Vizuete, A., and Gustafsson, J.-A. (1997), *J. Biol. Chem.* **272,** 2936–2941.
24. Lepiniec, L., Hodges, M., Gadal, P., and Cretin, C. (1992), *Plant Mol. Biol.* **18,** 1023–1025.
25. Lopez-Jaramillo, J., Chueca, A., Sahrawy, M., Hermoso, R., Lazaro, J. J., Prado, F. E., and Lopez-Gorge, J. (1994), *Plant Physiol.* **105,** 1021–1022.
26. Jacquot, J. P., Stein, M., Hodges, M., and Miginiac-Maslow, M. (1992), *Nucleic Acid Res.* **20,** 617.
27. Mittard, V., Morelle, N., Brutscher, B., Simorre, J. P., Marion, D., Stein, M., Jacquot, J.P ., Lirsac, P. N., and Lancelin, J. M. (1995), *Eur. J. Biochem.* **229,** 473–485.
28. Katti, S. K., Le Master, D. M., and Eklund, H. (1990), *J. Mol. Biol.* **212,** 167–184.
29. Saarinen, M., Gleason, F. K., and Eklund, H. (1995), *Structure* **3,** 1097–1108.
30. Mittard, V., Blackledge, M., Stein, M., Jacquot, J. P., Marion, D., and Lancelin, J. M. (1997), *Eur. J. Biochem.* **243,** 374–383.
31. Qin, J., Clore, G. M., Kennedy, W. M., Huth, J. R., and Gronenborn, A. M. (1995), *Structure* **3,** 289–297.
32. Janin, J. (1997), *Proteins* **28,** 153–161.
33. Demchuk, E., Mueller, T., Oschkinat, H., Sebald, W., and Wade R. (1994), *Protein Sci.* **3,** 920–935.
34. DePaskalis, A. R., Jelesarov, I., Ackermann, F., Koppenol, W. H., Hirasawa, M., Knaff, D. B., and Bosshard, H. R. (1993), *Protein Sci.* **2,** 1126–1135.
35. Gasdaska, J. R., Kirkpatrick, D. L., Montfort, W., Kuperus, M., Hill, S. R., Berggren, M., and Powis, G. (1997), *Biochem. Pharmacol.* **52,** 1741–1747.